ARCHIVES OF ACOUSTICS
32, 4, 941–954 (2007)

CRACK DETECTION ON BEAMS BY TIME-FREQUENCY ANALYSIS OF TRANSIENT FLEXURAL WAVES

Anastasia APOSTOLOUDIA[(1)], Evanthia DOUKA[(2)],
Leontios J. HADJILEONTIADIS[(3)], Ioannis T. REKANOS[(1)],
Athanasios TROCHIDIS[(1)]

Aristotle University of Thessaloniki

[(1)]Faculty of Engineering, Physics Division
GR-54124, Thessaloniki, Greece
e-mail: nataposto@yahoo.gr, rekanos@auth.gr, trohidis@gen.auth.gr

[(2)]Faculty of Engineering, Mechanics Division
e-mail: vanda@eng.auth.gr

[(3)]Faculty of Engineering
Department of Electrical and Computer Engineering
Division of Telecommunications
e-mail: leontios@auth.gr

(*received June 27, 2006; accepted June 21, 2007*)

A method for crack detection in beams by time-frequency analysis of flexural waves is described. Two different time-frequency representations, namely the continuous wavelet transform and the smoothed pseudo-Wigner distribution are employed. Simulated and measured flexural waves in a cracked beam are analysed and both the location and size of the crack are accurately determined. The location of the crack is estimated using the arrival time of reflected waves with different group velocities. The ratio of the reflected wave energy to the incident wave one is calculated and used as an indicator of the crack size. Wave experiments in a slender brass beam are in good agreement with predictions verifying the efficiency of the method. In view of the results obtained, the advantages and shortcomings of the time-frequency representations employed are presented and discussed.

Keywords: cracked beams, crack detection, wave propagation, time-frequency distributions, wavelets, Wigner distribution.

1. Introduction

Damage detection in structures is a problem of practical importance that has received considerable amount of interest during the last decades. As a result, a variety

of damage detection methods has been developed. Among the existing methods, wave-based techniques gained the ground. The basic concept, in most of these techniques, relies on the fact that a propagative wave will be reflected and partially transmitted when it encounters a defect. Measurements of the reflected and/or transmitted waves can provide significant information about the damage location and size. Unlike ultrasonic waves, middle frequency waves are not only sensitive to damage but also decay slowly; therefore, they are suitable for global inspection of structures. In that vein, flexural waves have been utilised for damage detection.

Since flexural waves are dispersive, a key issue in wave-based precise damage identification is the use of an appropriate method to analyse the measured signals and to extract their dispersive characteristics. Time-frequency analysis of dispersive waves allows the description of the time variation of each frequency component, offering several advantages in comparison to the traditional Fourier transform techniques.

So far, the continuous wavelet transform (CWT) [1] has been adopted for the analysis of guided waves because of its local and self-adaptive time-frequency resolution properties. ONSAY and HADDOW [2] examined the efficiency of the CWT in the analysis of impact-induced transient waves that propagate along a beam. They have demonstrated that the CWT is capable of analysing complex wave-interference patterns, which evolve over wide spectral ranges. INOUE *et al*. [3] applied the CWT to analyse the simulated flexural waves in an Euler–Bernoulli beam. They showed that the Gabor wavelet effectively decomposed the response into its time-frequency components and that the peaks of the time-frequency distribution indicate the arrival times of the waves. The same research group in a subsequent paper [4] experimentally verified their method by analysing flexural waves in a beam that resulted in the group velocity and impact site estimation. KIM and KIM [5] studied both analytically and experimentally the efficiency of the CWT to analyse the dispersive waves generated by an impact in a solid circular cylinder. They compared the performance of the CWT to that of the Short-Time Fourier transform and they pointed out the importance of choosing the appropriate wavelet to enhance the performance of the analysis. TIAN *et al*. [6] employed the CWT to analyse the flexural waves in a cracked Timoshenko beam. By identifying the arrival time of the waves with different group velocity, they were able to determine the location of the crack. QUEK *et al*. [7] applied the CWT to experimental data to locate a crack in a beam and discussed the impact of practical implementation issues, such as sampling rate, filtering and signal length, on the accuracy of the results. Recently, LI *et al*. [8] employed the CWT to identify both the location and depth of a crack in a cantilever beam. The crack depth was estimated by the value of the reflection and transmission ratios of the induced flexural waves. KIM and KIM [9] proposed a method for estimating damage location and size in a beam by analysing flexural waves. Using the CWT ridge analysis, the ratio of incident and reflected wave is estimated and correlated with the damage size.

In the present work, a method for estimating both the location and size of a crack in a beam by analysing transient flexural waves is presented. Two different time-frequency representations, namely the CWT and the smoothed pseudo-Wigner distribution (SPWD)

[10] for analysing the simulated and experimental signals are investigated. The objective is to compare their ability to resolve the dispersive characteristics of frexural waves. The location of the crack is estimated by calculating the arrival times of incident and reflected waves with different group velocities. The ratio of the reflected wave energy to the incident wave one is used as an estimator of the crack size. Experimental results in a brass beam have shown good agreement with predictions justifying the accuracy of the proposed method. The advantages and shortcomings of each time-frequency representation employed are compared and discussed.

2. Vibration model of a cracked infinite beam

A beam of infinite length along the x axis, with uniform rectangular cross-section $w \times w$, which has a transverse surface crack located at the origin of the x axis (Fig. 1), is considered. The beam is excited by a force whose Fourier transform is $F(\omega)$. The force acts at a distance L from the crack position. For the solution of the displacement along the beam, the spectral analysis is adopted where the time dependence has the form $\exp(j\omega t)$. In particular, for each frequency ω the harmonic solution of the displacement $n(x,\omega)$ for the three regions defined along the beam is given by

$$\begin{aligned} R_1 &= \{x\colon x \le -L\}; & n_1(x,\omega) &= A_1^-(\omega)\mathrm{e}^{jkx} + B_1^-(\omega)\mathrm{e}^{kx}; \\ R_2 &= \{x\colon -L \le x \le 0\}; & n_2(x,\omega) &= A_2^+(\omega)\mathrm{e}^{-jkx} + B_2^+(\omega)\mathrm{e}^{-kx} \end{aligned} \tag{1}$$

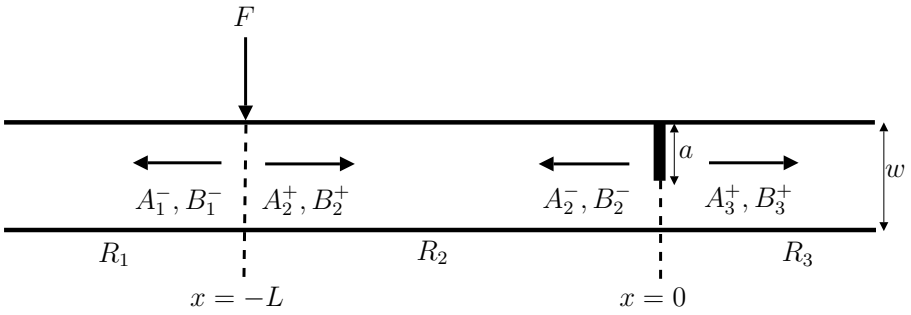

Fig. 1. Geometry of the cracked infinitely long beam under study.

In Eq. (1), the A and B coefficients are related to travelling and evanescent waves, respectively. The subscripts refer to the corresponding regions along the beam, whereas the plus and minus superscripts denote propagation along the positive and negative x direction, respectively. Finally, the wavenumber k that appears in Eq. (1) is derived by

the Euler–Bernoulli model and is given by

$$k = \left[\omega^2 \frac{\rho S}{EI}\right]^{1/4}, \tag{2}$$

where ρ is the mass density, S is the cross-sectional area, E is the Young's modulus, and I is the moment of inertia of the beam.

The evaluation of the unknown A and B coefficients is based on the fulfilment of boundary conditions at the locations of the impact and the crack. At the impact location ($x = -L$) the continuity of displacement, gradient of displacement, moment and shear are imposed, resulting in four equations, i.e.,

$$\begin{aligned} n_1(-L,\omega) &= n_2(-L,\omega), \\ \partial_x n_1(-L,\omega) &= \partial_x n_2(-L,\omega), \\ \partial_x^2 n_1(-L,\omega) &= \partial_x^2 n_2(-L,\omega), \\ \partial_x^3 n_2(-L,\omega) - \partial_x^3 n_1(-L,\omega) &= F/(EI). \end{aligned} \tag{3}$$

At the crack location ($x = 0$) the continuity of displacement, moment and shear are imposed, resulting in three equations

$$n_2(0,\omega) = n_3(0,\omega), \quad \partial_x^2 n_2(0,\omega) = \partial_x^2 n_3(0,\omega), \quad \partial_x^3 n_2(0,\omega) = \partial_x^3 n_3(0,\omega), \tag{4}$$

respectively. Furthermore, the crack can be modelled by a massless rotational spring, whose bending stiffness K_T is given by [11]

$$K_T = 0.1871 \frac{EI}{wJ(a/w)}, \tag{5}$$

where a is the depth of the crack and $J(a/w)$ is the dimensionless local compliance function given by

$$\begin{aligned} J(u) &= 1.98u^2 - 3.277u^3 + 14.43u^4 - 31.26u^5 + 63.56u^6 \\ &\quad - 103.36u^7 + 147.52u^8 - 127.69u^9 + 61.5u^{10}. \end{aligned} \tag{6}$$

Under this assumption, an additional boundary condition, which is related to the equilibrium between transmitted bending moment and spring rotation, is imposed at the crack location, i.e.,

$$-EI\partial_x^2 n_2(0,\omega) = K_T[\partial_x n_2(0,\omega) - \partial_x n_3(0,\omega)]. \tag{7}$$

By solving the system of the eight Eqs. (3), (4), and (7), the A and B coefficients are evaluated. In particular, after some manipulation, the coefficients related to the wave travelling toward the crack (region R_2) are given by

$$A_2^+(\omega) = -j\frac{F}{4EIk^3}\mathrm{e}^{-jkL}, \qquad B_2^+(\omega) = -\frac{F}{4EIk^3}\mathrm{e}^{-kL}. \tag{8}$$

The coefficients associated with the wave reflected from the crack are related to the incident wave ones through the reflection matrix $\mathbf{R}(\omega)$, i.e.,

$$\begin{bmatrix} A_2^-(\omega) \\ B_2^-(\omega) \end{bmatrix} = \mathbf{R}(\omega) \begin{bmatrix} A_2^+(\omega) \\ B_2^+(\omega) \end{bmatrix}. \tag{9}$$

The reflection matrix, which depends on the properties of the crack is given by

$$\mathbf{R}(\omega) = -\frac{\tilde{k}}{\tilde{k}(1-j)-4j}\begin{bmatrix} 1 & -1 \\ j & -j \end{bmatrix}, \tag{10}$$

where $\tilde{k} = EIk/K_T$.

Furthermore, the coefficients of the wave transmitted through the crack in region R_3 are given by

$$\begin{bmatrix} A_3^+(\omega) \\ B_3^+(\omega) \end{bmatrix} = (\mathbf{I} + \mathbf{R}(\omega)) \begin{bmatrix} A_2^+(\omega) \\ B_2^+(\omega) \end{bmatrix}, \tag{11}$$

where $\mathbf{I}$ is the unit matrix. The sum of the unit matrix and the reflection matrix is interpreted as the transmission matrix $\mathbf{T}(\omega) = \mathbf{I} + \mathbf{R}(\omega)$.

Finally, the coefficients of the wave travelling in region R_1 are given by

$$\begin{bmatrix} A_1^-(\omega) \\ B_1^-(\omega) \end{bmatrix} = \begin{bmatrix} \mathrm{e}^{2jkL} & 0 \\ 0 & \mathrm{e}^{2kL} \end{bmatrix} \begin{bmatrix} A_2^+(\omega) \\ B_2^+(\omega) \end{bmatrix} + \begin{bmatrix} A_2^-(\omega) \\ B_2^-(\omega) \end{bmatrix}. \tag{12}$$

After the evaluation of the A and B coefficients, the displacement in the time domain, $n(x,t)$, can be obtained by applying the inverse Fourier transform to $n(x,\omega)$. For example, according to Eq. (1), the displacement at any position x in region R_2 is given by

$$\begin{aligned} n_2(x,t) \;=\; & \frac{1}{2\pi}\int_{-\infty}^{+\infty}\Big[A_2^+(\omega)\mathrm{e}^{-jkx} + B_2^+(\omega)\mathrm{e}^{-kx} \\ & + A_2^-(\omega)\mathrm{e}^{jkx} + B_2^-(\omega)\mathrm{e}^{kx}\Big]\mathrm{e}^{j\omega t}\,\mathrm{d}\omega, \end{aligned} \tag{13}$$

while the associated acceleration $\gamma_2(x,t)$ is obtained as

$$\gamma_2(x,t) = -\frac{1}{2\pi}\int_{-\infty}^{+\infty}\omega^2 n_2(x,\omega)\mathrm{e}^{j\omega t}\,\mathrm{d}\omega. \tag{14}$$

3. Estimation of the reflection coefficient

From the analysis presented in the previous section, it is evident that the acceleration in the time domain at any position along the beam depends on the location and size of the crack. In particular, if the impact is impulsive and the acceleration is evaluated at any position in region R_2, then the acceleration signal is composed of two parts; the first, in time, corresponds to the incident wave generated by the impact, while the second one is generated by the crack because of the reflection. In general, the reflected signal is lower than the incident one and its relative amplitude is governed by the size of the crack.

The characteristics of the crack, i.e. location and size, are introduced to the evaluation of the acceleration through the elements of the reflection matrix (Eq. (10)). Furthermore, since the evanescent waves related to the B coefficients do not significantly contribute to the acceleration, we conclude from Eq. (9) that the (1,1) element of the reflection matrix

$$\mathbf{R}_{11}(\omega) = -\frac{\tilde{k}}{\tilde{k}(1-j)-4j}, \tag{15}$$

which is considered in the following as the *reflection coefficient*, can be estimated by means of the travelling wave phasors A_2^- and A_2^+, i.e.,

$$\widehat{\mathbf{R}}_{11}(\omega) = A_2^-(\omega)/A_2^+(\omega). \tag{16}$$

Alternatively, the magnitude of the reflection coefficient can be derived from

$$|\widehat{\mathbf{R}}_{11}(\omega)| = \left(\frac{E_r(\omega)}{E_i(\omega)}\right)^{1/2}, \tag{17}$$

where $E_i(\omega)$ and $E_r(\omega)$ are the incident and the reflected energy from the crack, respectively, at frequency ω.

Clearly, the estimation of the reflection coefficient or of its magnitude requires the identification and separation of the incident and the reflected waves travelling in region R_2. This problem can be coped with by utilising time analysis of the acceleration signals. Furthermore, due to the dispersion involved, the waveform of the incident signal is not preserved in the reflected signal. Hence, to analyse the acceleration signal, the time-frequency analysis is utilised.

In the following, the strategy adopted for estimation of the location of the crack and estimation of the reflection coefficient magnitude, is presented by means of a characteristic example. Let us consider again a cracked infinite beam shown in Fig. 1, which is impacted by a delta Dirac force. The acceleration is evaluated at a position in region R_2 placed at a distance L_M from the crack. A typical simulated acceleration signal is illustrated in Fig. 2a. The parts of the signal related to the incident and the reflected waves are pointed in Fig. 2a by arrows. The dispersive character of the wave propagating in the beam is evident by comparing the form and the duration of the incident and the reflected waves. The dispersion can also be shown by means of time-frequency representation of the signal. In particular, the CWT of the signal is presented in the time-frequency plane in Fig. 2b, where the ridges related to the incident and the reflected waves are also depicted by arrows.

Post-processing of the time-frequency representation could result in estimating the reflection coefficient spectrum. For example, the estimation of the magnitude of the reflection coefficient at frequency ω_0 is derived from the time variation of the wavelet coefficient magnitude, $|W(t,\omega_0)|$, corresponding to frequency ω_0. This variation is illustrated in Fig. 2c for frequency equal to 10 kHz. From Fig. 2c, the time durations ΔT_i and ΔT_r of the incident and the reflected waves, respectively, are obtained. Hence,

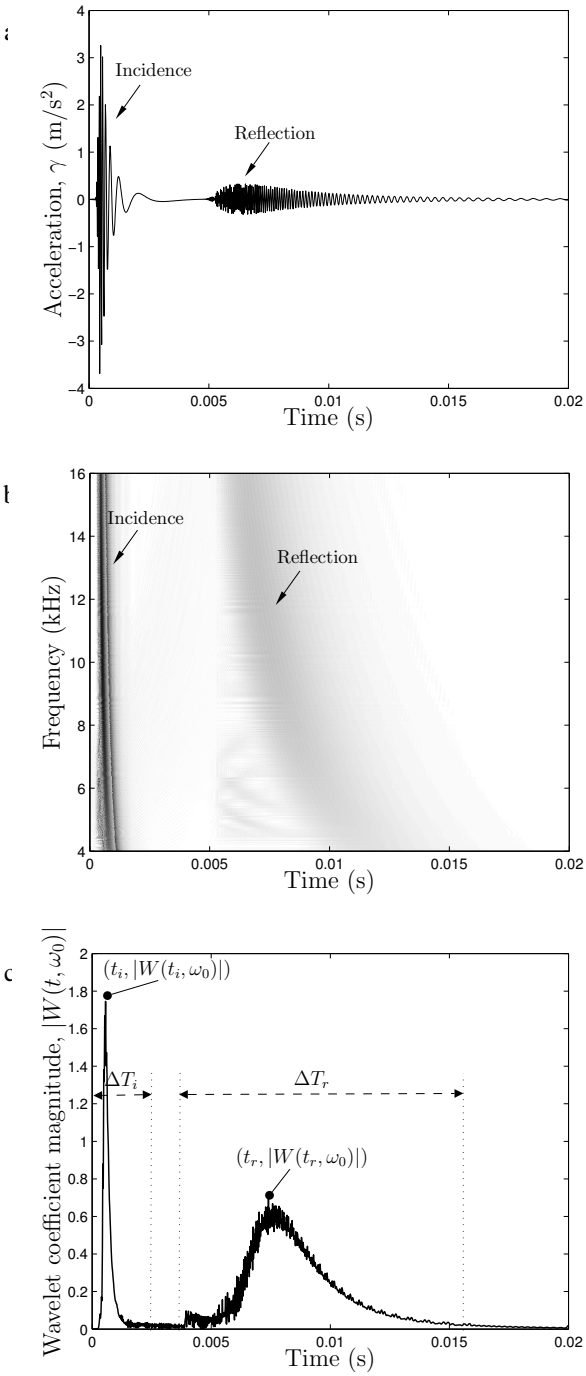

Fig. 2. a) Typical simulated acceleration signal. b) Time-frequency representation of the wavelet coefficients magnitude of the acceleration signal. c) Time variation of the wavelet coefficient magnitude, for frequency equal to 10 kHz.

according to Eq. (17), the estimate of the reflection coefficient magnitude is given by

$$|\widehat{\mathbf{R}}_{11}(\omega_0)| = \left(\frac{\int\limits_{\Delta T_r} |W(t,\omega_0)|^2 \, \mathrm{d}t}{\int\limits_{\Delta T_i} |W(t,\omega_0)|^2 \, \mathrm{d}t} \right)^{1/2} . \tag{18}$$

This energy-based approach for the estimation of $|\mathbf{R}_{11}(\omega_0)|$ is adopted to compensate for the dispersion effect, since the energy associated with each distinct frequency is spread in time. On the contrary, if the maximum values $|W(t_i,\omega_0)|$ and $|W(t_r,\omega_0)|$ of the incident and the reflected wave, respectively, are used in Eq. (16) to estimate $|\mathbf{R}_{11}(\omega_0)|$ [8, 9], i.e.,

$$|\widehat{\mathbf{R}}_{11}(\omega_0)| = |W(t_r,\omega_0)|/|W(t_i,\omega_0)|, \tag{19}$$

then the estimation is less accurate, since dispersion effects are neglected. It should be noted that Eq. (19) could be applicable in non-dispersive cases.

Determining the time instances $t_i(\omega_0)$ and $t_r(\omega_0)$ of maximum values $|W(t_i,\omega_0)|$ and $|W(t_r,\omega_0)|$ is helpful in estimating the location of the crack. These time instances represent the arrival times of the incident and the reflected waves, respectively. Thus, if the group velocity $c_g(\omega_0)$ is known, then the estimate of the distance between the measurement position and the crack is given by

$$\widehat{L}_M = \frac{t_r(\omega_0) - t_i(\omega_0)}{2c_g(\omega_0)} . \tag{20}$$

4. Simulated results

For numerical simulations, an infinite brass beam of rectangular cross-section $S = 0.016 \times 0.016$ m^2 with modulus of elasticity $E = 97.66$ GPa and mass density $\rho = 8500$ kg/m^3 is considered. A crack of varying depth is introduced and the beam is impacted by a delta Dirac force at a distance $L = 8$ m from the crack location. The assumption of an infinite beam is adopted in order to avoid multiple reflections from the boundaries. The acceleration response of the beam is evaluated at a position $L_M = 7$ m from the crack, based on the theoretical model presented in Sec. 2.. Actually, the signal presented in Fig. 2a has been obtained by the model, for the case of relative crack depth of 40%. Following the initial occurrence of the impulse (incident wave), a period of time (0.0055–0.02 s) is observed (see Fig. 2a), during which the wave reflected from the crack travels back.

The signal analysis is aiming at relating the characteristics of the reflected wave to the crack size. To this end, simulated acceleration signals are calculated for relative crack depths of 10%–40% in steps of 10%, using a sampling frequency of 51200 Hz. Each case is analysed using two methods, namely CWT and SPWD, in order to obtain the time-frequency distributions. The curves of the reflection coefficient magnitude, for all crack depths considered, are predicted in the [4–16 kHz] frequency range by using

the formula

$$|\widehat{\mathbf{R}}_{11}(\omega)| = \left(\frac{\int\limits_{\Delta T_r} P(t,\omega)\,\mathrm{d}t}{\int\limits_{\Delta T_i} P(t,\omega)\,\mathrm{d}t} \right)^{1/2}, \tag{21}$$

where P is the power distribution derived by each method. The results for the methods examined are shown in Fig. 3.

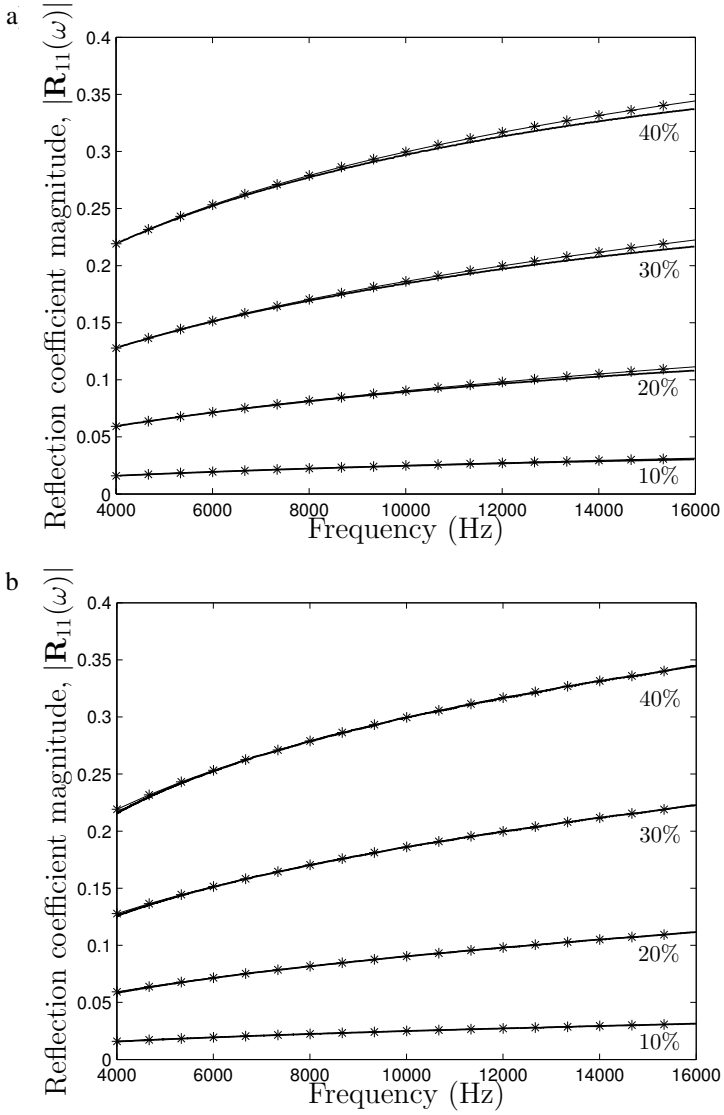

Fig. 3. Estimated reflection coefficient magnitude vs. frequency, based on simulated signals for relative crack depths of 10%, 20%, 30%, and 40%. Results derived by a) CWT and b) SPWD. Lines with asterisks stand for the theoretical results derived from Eq. (15).

For comparison reasons, the theoretical curves of the reflection coefficient derived from Eq. (15) are also depicted. The reflection coefficients predicted through the CWT analysis, shown in Fig. 3a, follow the theoretical curves consistently for all crack depths and over the entire frequency-range involved. Figure 3b presents the results derived by the SPWD method. The estimated reflection coefficient magnitude is in excellent agreement with the theory.

5. Experimental results

The experimental arrangement is shown in Fig. 4. It consisted of a uniform brass beam of cross-section $S = 0.016 \times 0.016$ m^2, a total length of $L = 3$ m and material properties $E = 97.66$ GPa and $\rho = 8500$ kg/m^3. The beam was suspended horizontally by thin threads at a distance $L/10$ away from the ends to approximate the free-free boundary conditions. A saw cut was introduced at $x_c = 1.01$ m from the left end to simulate the transverse crack. A miniature accelerometer was mounted at $x_a = 0.01$ m from the left free end to measure the response of the beam. The beam was excited by the impact of a steel ball (diameter 6 mm) dropped from a constant height at the left free end. Flexural waves generated by the impact were measured, recorded in a computer and later analysed.

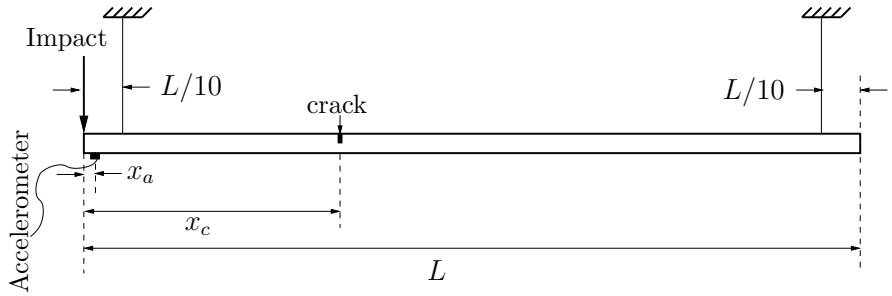

Fig. 4. Experimental arrangement.

Experiments were performed for three different relative crack depths, namely 10%, 20% and 30% and the corresponding spectra were obtained by application of the two time-frequency methods. In this analysis, both the reflection coefficient magnitude and the location of the crack are to be estimated.

Following the procedure described in the simulated results (Sec. 4), the reflection coefficients are predicted and the results are shown in Fig. 5, where the theoretical curves are also depicted. It can be observed from Figs. 5a and 5b that both CWT and SPWD give similar results, with the SPWD curves being slightly closer to the theoretical ones (for relative crack depths of 20% and 30%). The predicted curves seem to deviate from the theoretical ones, for all crack depths, mainly because of the frequency content of the beam impact that differs from that of a pure impulse. Moreover, the theoretical reflection coefficient curves are derived, based on the Euler–Bernoulli beam theory that is an approximation model.

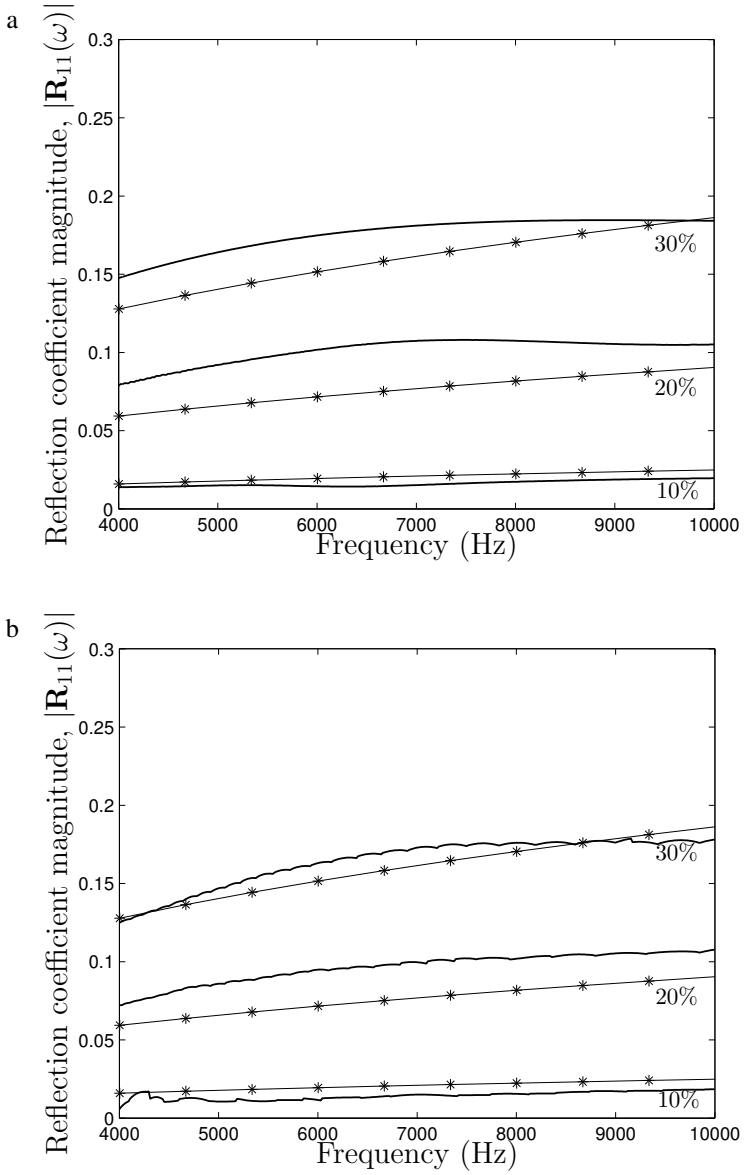

Fig. 5. Estimated reflection coefficient vs. frequency, based on experimental signals for relative crack depths of 10%, 20%, and 30%. Results derived by a) CWT and b) SPWD. Lines with asterisks stand for the theoretical results derived from Eq. (15).

In order to estimate the location of the crack, the frequency-dependent group velocity of the specific beam is obtained experimentally by exciting a healthy beam of the same characteristics. Through the time-frequency distribution of each method, the arrival times associated with the impact and the first boundary reflection are identified

as the time instances that correspond to the maximum values of the power distribution for each frequency. The group velocity is determined as

$$c_g(\omega) = \frac{2L_B}{t_b(\omega) - t_i(\omega)}\,, \tag{22}$$

where L_B is the distance between the measurement position and the boundary of the beam, while t_b and t_i denote the arrival times of the reflected and the incident waves, respectively.

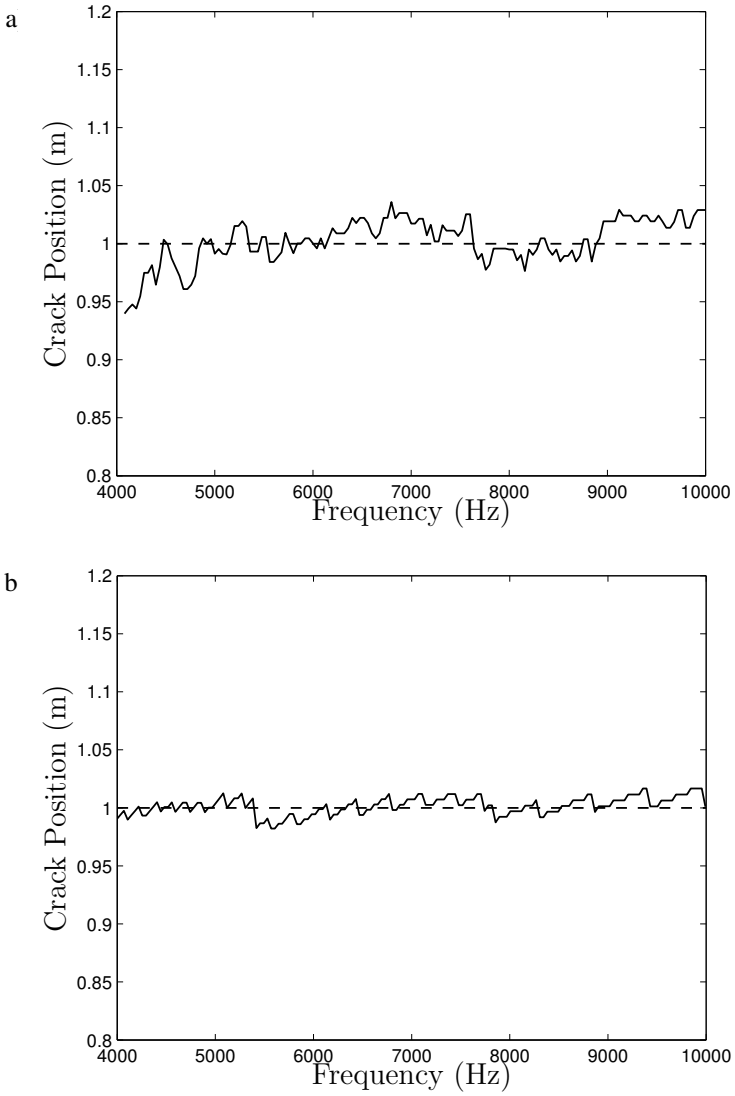

Fig. 6. Estimated crack position vs. frequency, based on experimental signals for relative crack depth of 20%. Results derived by a) CWT and b) SPWD. Dashed line represents the real crack position, $L_M = 1$ m.

The derived group velocity is utilised in Eq. (20) to estimate the location of the crack, namely the distance between the accelerometer and the crack. Note that in the experimental arrangement, the real location of the crack is $L_M = x_c - x_a = 1$ m. Figure 6 illustrates the estimated crack locations vs. the frequency for the two methods examined, in the case of relative crack depth of 20%, while Table 1 presents the mean and the standard deviation of the absolute error of the estimated crack location for all crack depth cases. From these results we conclude that the SPWD performs better than the CWT, giving accurate predictions of the crack location.

Table 1. Mean value $\bar{\epsilon}$ and standard deviation σ_ϵ of the absolute error of the estimated crack location derived by the two methods examined: Continuous Wavelet Transform (CWT) and Smoothed Pseudo-Wigner Distribution (SPWD). Results are obtained from experimental signals and for relative crack depths of 10%, 20%, and 30%.

Crack Depth	10%		20%		30%	
	$\bar{\epsilon}$	σ_ϵ	$\bar{\epsilon}$	σ_ϵ	$\bar{\epsilon}$	σ_ϵ
CWT	0.0211	0.0147	0.0175	0.0127	0.0155	0.0115
SPWD	0.0069	0.0048	0.0064	0.0045	0.0063	0.0044

6. Conclusions

In this paper, two time-frequency representation methods (CWT and SPWD) were employed for detecting the cracks in beams. The size of the crack was associated with the reflected coefficient magnitude, which is evaluated by considering the ratio of the energy reflected by the crack to the incident energy generated by an impact. The energies carried by forward and backward travelling transient flexural waves were evaluated for each excitation frequency over a wide range of frequencies. Furthermore, the location of the crack with respect to the acceleration measurement position was estimated, based on the difference between time arrivals of the incident and the reflected waves.

The performance of each method was investigated by means of both the simulated and experimental data. Results indicate that the SPWD provides the best performance in accurately estimating both the reflection coefficient magnitude and the location of the crack. The results derived by the CWT were also reliable. However, the SPWD outperforms the CWT, because the SPWD results in finer resolution in the time-frequency plane giving concentrated (narrow) ridges; thus, the evaluation of both the energy and arrival times is more accurate.

Concluding, among the methods examined, the SPWD is the most accurate and reliable one for crack detection based on wave propagation of transient flexural waves. Also, the CWT performs well, while its accuracy could be further improved by appropriate selection of the mother wavelet used.

Acknowledgment

This work was supported by the Greek General Secretariat of Research and Technology through Grant 01EΔ330.

References

[1] MALLAT S., *Wavelet Tour of Signal Processing*, Academic Press, New York 1998.

[2] T. ONSAY, A. G. HADDOW, *Wavelet transform analysis of transient wave propagation in a dispersive medium*, Journal of the Acoustical Society of America, **95**, 3, 1441–1449 (1994).

[3] H. INOUE, K. KISHIMOTO, T. SHIBUYA, *Experimental wavelet analysis of flexural waves in beams*, Experimental Mechanics, **36**, 3, 212–217 (1996).

[4] K. KISHIMOTO, H. I. M. HAMADA, T. SHIBUYA, *Time-frequency analysis of dispersive waves by means of wavelet transform*, Journal of Applied Mechanics, Transactions of the ASME, **62**, 4, 841–846 (1995).

[5] Y. Y. KIM, E. H. KIM, *Effectiveness of continuous wavelet transform in the analysis of some elastic dispersive waves*, Journal of the Acoustical Society of America, **110**, 1, 86–94 (2001).

[6] J. Y. TIAN, Z. LI, X. SU, *Crack detection in beams by wavelet analysis of transient flexural waves*, Journal of Sound and Vibration, **261**, 4, 715–727 (2003).

[7] S. T. QUEK, Q. WANG, L. ZHANG, K. H. ONG, *Practical issues in the detection of damage in beams using wavelets*, Smart Materials and Structures, **10**, 5, 1009–1017 (2001).

[8] Z. LI, S. XIA, J. WANG, X. SU, *Damage detection of cracked beams based on wavelet transform*, International Journal of Impact Engineering, **32**, 7, 1190–1200 (2006).

[9] I. K. KIM, Y. Y. KIM, *Damage size estimation by the continuous wavelet ridge analysis of dispersive bending waves in beam*, Journal of Sound and Vibration, **287**, 4-5, 707–722 (2005).

[10] COHEN L., *Time-frequency distributions – a review*, Proceedings of the IEEE, **77**, 7, 941–981 (1989).

[11] OKAMURA H., LIU H. W., SHU C.-S., LIEBOWITZ H., *A cracked column under compression*, Engineering Fracture Mechanics, **1**, 3, 547–564 (1969).